JOURNAL OF SOLID STATE CHEMISTRY 96, 123–131 (1992)

Chemical Synthesis and Properties of $Li_{1-\delta-x}Ni_{1+\delta}O_2$ and $Li[Ni_2]O_4$

G. DUTTA, A. MANTHIRAM, AND J. B. GOODENOUGH

Center for Materials Science & Engineering, ETC 5.160, University of Texas at Austin, Austin, Texas 78712-1084

AND J.-C. GRENIER

Laboratoire de Chimie du Solide du CNRS, 351, cours de la Libération, 33405 Talence Cedex, France

Received July 29, 1991

DEDICATED TO PROFESSOR PAUL HAGENMULLER

Magnetic and transport properties of the layered ($R\bar{3}m$) metastable system $Li_{1-\delta-x}Ni_{1+\delta}O_2$ and the cubic spinel $Li[Ni_2]O_4$ are reported for samples prepared from $(Li_{1-\delta}Ni_\delta)NiO_2$, $\delta = 0.04$ and 0.08, by chemical extraction of lithium with NO_2PF_6 at room temperature. Transformation of the layered phase to the cubic spinel was accomplished by heating $(\delta + x) \approx 0.5$ samples to 250–300°C in an evacuated, sealed quartz tube. These mixed-valent compounds are small-polaron semiconductors, and the low-spin Ni^{3+} ions carry a nickel magnetic moment close to 1 μ_B; the low-spin Ni^{4+} ions are diamagnetic. The magnetic interactions are those predicted for partially filled crystal-field orbitals of e parentage, which are associated with σ bonding in octahedral sites. Nevertheless, there is no cooperative Jahn–Teller distortion of the type expected for strong Jahn–Teller ions with localized e-orbital configurations in octahedral sites. These findings cast doubt on any interpretation of these oxides that leaves unmodified the magnitude of the Hubbard U and the positions of the redox energies from their values in NiO.

1. Introduction

Antiferromagnetic NiO is well described (*1*) by an ionic model in which the covalent Ni–O mixing is taken into account via second-order perturbation theory within the crystal-field description of the localized "3*d*" electrons. In this model, the Ni–Ni and Ni–O–Ni interactions are then described by the second-order superexchange perturbation, and an important distinction is made between Ni–Ni and Ni–O–Ni interactions. Although the strong Ni–O–Ni interactions appear to approach the condition for a transition from localized-electron to itinerant-electron antiferromagnetism, nevertheless the ionic model provides a satisfactory description of the ground-state properties of stoichiometric NiO.

On the other hand, problems begin with the use of an ionic model to interpret the spectroscopic data (*2*); the conclusion that NiO has a charge-transfer rather than a "correlation" energy gap implies—within the ionic model—that, on oxidation, holes are introduced into a band of primarily O-2*p* character rather than into one of primarily Ni-3*d* character. Earlier observation (*3*) that

0022-4596/92 $3.00

mobile holes introduced into NiO have an itinerant-electron character (the mobility has no activation energy) had already encouraged such a conclusion (*4*). Yet, electrochemical data on, for example, the nickel electrode of a Cd–Ni cell imply the presence of a well-defined $Ni^{3+/2+}$ couple—at least at the surface—of $NiO_{2-x}(OH)_x$, $1 < x < 2$ (*5*). If the situation appears ambiguous for the $Ni^{3+/2+}$ couple, then how should we think about the mixed-valent oxides having, formally, a $Ni^{4+/3+}$ redox couple? The problem thus raised is particularly germane to our description of the high-T_c copper-oxide superconductors.

In this paper we explore experimentally the systems $Li_{1-x}NiO_2$ and $Li[Ni_2]O_4$ containing, formally, the mixed-valent redox couple $Ni^{4+/3+}$. We distinguish the 90° Ni–O–Ni interactions occurring in these compounds from the 180° Ni–O–Ni interactions found in the metallic, Pauli paramagnetic perovskite $LaNiO_3$.

2. Experimental

2.1. Chemical Synthesis

The nominal parent compound $LiNiO_2$ was prepared in two ways. In the first method, stoichiometric amounts of NiO and Li_2CO_3 were ground finely in an agate mortar to form a homogeneous mixture. The mixture was heated at 500°C for 5 h before the temperature was slowly raised to 900°C. After the mixture was heated at 900°C for 48 h with intermittent grinding, the X-ray powder diffraction indicated a single-phase product. In the second method, Li_2CO_3 was dissolved in dilute nitric acid; nickel acetate was added in appropriate proportion and stirred until a clear solution formed. This solution was heated slowly to evaporate the water; the dried mixture was transferred to an alumina boat, heated at 500°C for 5 h, and finally fired at 700°C for 24 h to form $LiNiO_2$. The first method yielded a highly sintered compound having the composition $Li_{0.96}Ni_{1.04}O_2$; the second gave a soft product with the composition $Li_{0.92}Ni_{1.08}O_2$.

Chemical extraction of lithium from these parent compositions was carried out with the oxidizing agent NO_2PF_6 in acetonitrile under an argon atmosphere:

$$Li_{1-\delta}Ni_{1+\delta}O_2 + xNO_2PF_6 \xrightarrow{CH_3CN} Li_{1-\delta-x}N_{1+\delta}O_2 + xNO_2 + xLiPF_6. \quad (1)$$

$LiPF_6$ is soluble in acetonitrile; the oxide product remains behind as the only solid phase. The product was washed several times with acetonitrile and dried in vacuum; it was then stored in an argon-filled glove box.

The reaction of $Li_{1-\delta}Ni_{1+\delta}O_2$ with NO_2PF_6 is not 100% efficient, and excess NO_2PF_6 had to be used. Also, some of the $Li_{1-\delta-x}Ni_{1+\delta}O_2$ decomposes into solution, as is made evident by the blue color of the filtrate. The experiment was repeated at 60°C and also in an ice bath with no improvement in the yield. At 60°C, the reaction was vigorous and the product was not a single phase. At lower temperatures the reaction did not occur. The $Li_{1-\delta-x}Ni_{1+\delta}O_2$ compositions obtained from $Li_{0.96}Ni_{1.04}O_2$ fell in the range $0.0 \leq x \leq 0.40$; on the other hand, a composition $Li_{0.32}Ni_{1.08}O_2$ was obtained as a single phase from the $Li_{0.92}Ni_{1.08}O_2$ parent compound.

The spinel $Li[Ni_2]O_4$ had already been prepared from a nominal $Li_{0.5}NiO_2$ sample prepared electrochemically (*6*); the spinel is only stable below 300°C, and a temperature of 250°C is needed to transform metastable $Li_{0.5}NiO_2$ to $Li[Ni_2]O_4$. Since we found it difficult to obtain chemically the exact stoichiometry $Li_{0.5}NiO_2$, we proceeded to make nominal $Li[Ni_2]O_4$ by two methods. In one we started with a sample analyzing as $Li_{0.58}Ni_{1.04}O_2$; in the other we used a calculated mixture of $Li_{0.5+\xi}NiO_2$ and $Li_{0.5-\eta}NiO_2$ corresponding to a net $Li_{0.5}NiO_2$. Each type

of sample was pelletized and heated in an evacuated, sealed quartz tube at temperatures 250–300°C for several days.

2.2 Characterization

All samples were stored in an argon-filled glove box. They were characterized by X-ray powder diffraction recorded with a Philips diffractometer. Li contents were determined with a Perkin–Elmer 1100 Atomic Absorption Spectrophotometer. Resistance measurements were made on sintered pellets with a two-probe method; magnetic-susceptibility data were obtained in Bordeaux with an automatic susceptometer (DSM8-type, MAVICS) at 1.8 T.

3. Results and Discussion

3.1 Structural Considerations

The parent compositions $Li_{1-\delta}Ni_{1+\delta}O_2$, $\delta = 0.04$ and 0.08, have a layered structure isomorphous with that of α-$NaFeO_2$ (*7*). The (111) octahedral-site planes of a face-centered-cubic oxide-ion array would be occupied alternately by Li^+ and Ni^{3+} ions in stoichiometric $LiNiO_2$. It was already noted many years ago (*8*) that stoichiometric $LiNiO_2$ is extremely difficult to prepare; magnetic and density measurements also showed that the lithium deficiency is not due to Li^+-ion vacancies in the lithium layers, but to the presence of excess nickel occupying Li^+-ion sites. Thus the parent compounds $\delta = 0.04$ and 0.08 have the compositions $(Li^+_{0.96}Ni^{2+}_{0.04})(Ni^{3+}_{0.96}Ni^{2+}_{0.04})O_2$ and $(Li^+_{0.92}Ni^{2+}_{0.08})(Ni^{3+}_{0.92}Ni^{2+}_{0.08})O_2$, respectively. This situation places the Fermi energy E_F of the parent compositions in the $Ni^{3+/2+}$ couple rather than the $Ni^{4+/3+}$ couple.

The layered structure makes possible the room-temperature extraction of lithium; the Li^+ ions are mobile at room temperature in such an oxide. However, extraction of lithium requires moving E_F from the $Ni^{3+/2+}$ couple to the $Ni^{4+/3+}$ couple, which is itself highly oxidizing. It is therefore difficult to find a strong enough oxidant to extract Li from $Li_{1-\delta}Ni_{1+\delta}O_2$ chemically with 100% efficiency. Consequently initial experiments (*6, 9*) used electrochemical lithium extraction. However, this method yields small samples that may be inhomogeneous, so physical measurements were not attempted. Recently, Wizansky *et al.* (*10*) have reported the chemical extraction of lithium from $LiCoO_2$ with the oxidizing agents NO_2PF_6 and MoF_6. This report prompted our use of NO_2PF_6 as the oxidizing reagent for extracting lithium chemically from the parent compounds $Li_{1-\delta}Ni_{1+\delta}O_2$, $\delta = 0.04$ and 0.08. Although the reaction was not 100% efficient, it did permit the preparation of samples $Li_{1-\delta-x}Ni_{1+\delta}O_2$ and $Li[Ni_2]O_4$ in sufficient quantity for physical measurements to be made.

Figure 1 shows the variation of lattice parameters with x for $Li_{1-\delta-x}Ni_{1+\delta}O_2$; the $0 \leq x \leq 0.40$ samples were obtained by lithium extraction from $Li_{0.96}Ni_{1.04}O_2$ while the $x > 0.45$ samples were obtained from $Li_{0.92}Ni_{1.08}O_2$. The decrease in the a parameter with decreasing Li^+-ion concentration reflects the decrease in Li^+–Li^+ electrostatic repulsion within a basal plane as well as the smaller effective size of a Li^+-ion vacancy; the increase in the c parameter reflects the electrostatic repulsion between oxide–ion planes as the positive charge between these planes is decreased. The change in slope of a vs x at $x \approx 0.45$, which corresponds to $x + \delta \approx 0.05$, may reflect primarily a Li^+-ion ordering, but it also appears to reflect some irreversible displacement of nickel to the Li-atom planes (see below).

The open-circuit voltage V_{oc} versus a lithium anode is also shown in Fig. 1 for $Li_{0.96-x}Ni_{1.04}O_2$ as a function of x. In the range $0.0 \leq x \leq 0.46$, the V_{oc} vs x curve increases linearly; for $x > 0.46$ it remains constant. However, the lattice parameters vary con-

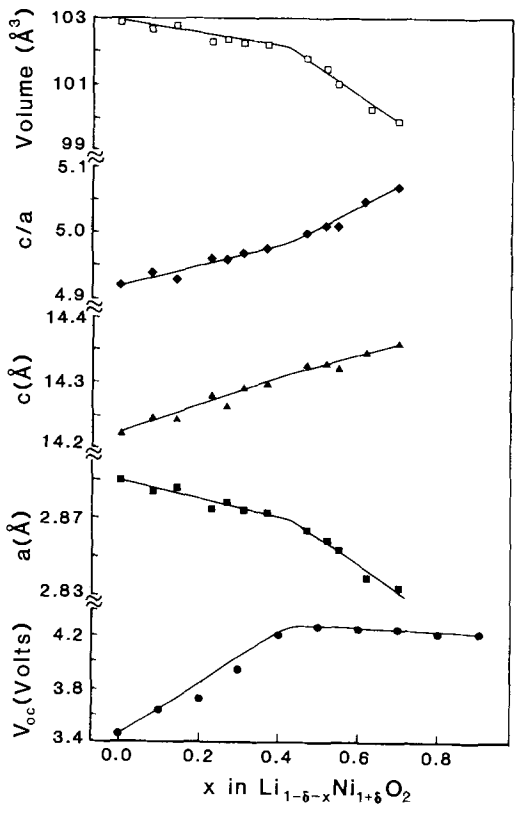

FIG. 1. Variation of lattice parameters and open-circuit voltage with x for $Li_{1-\delta-x}Ni_{1+\delta}O_2$. The lattice parameters plotted correspond to $Li_{0.96-x}Ni_{1.04}O_2$ for $0 \leq x \leq 0.40$ and to $Li_{0.92-x}Ni_{1.08}O_2$ for $x > 0.45$. The open-circuit voltages correspond to $Li_{0.96-x}Ni_{1.04}O_2$ for $0 \leq x \leq 0.95$.

tinuously with x without any evidence for two crystallographic phases in this range on chemical delithiation. Two explanations are plausible for $x > 0.46$: either the open-circuit voltage becomes so large that the electrolyte is oxidized or the displacement of nickel to the Li-atom planes is controlled by the retention of a constant Fermi energy without the formation of a discrete second phase.

The powder X-ray diffraction profiles for $Li_{0.96}Ni_{1.04}O_2$ and $Li_{0.58}Ni_{1.04}O_2$ of Fig. 2(a) and (b) show a large decrease in the intensities of the peaks with increasing x, but the intensity of the critical (003) peak remains unchanged, which is unlike the case of $Li_{1-x}VO_2$ with $x > 0.33$ (*11*) where V atoms are displaced to the Li-atom planes. There is no evidence of a significant nickel-atom displacement to the Li-atom planes over the range $0 \leq x \leq 0.38$ in $Li_{0.96-x}Ni_{1.04}O_2$. The changes in peak intensities may reflect problems with preferred orientation. Since a displacement of the transition-metal atoms from one octahedral-site (111) plane to the next is via a tetrahedral site, the greater metastability of nominal $Li_{1-x}NiO_2$ relative to $Li_{1-x}VO_2$ can be understood. The disproportionation reaction $2V^{4+} \rightarrow V^{5+} + V^{3+}$ requires little energy, and the V^{5+} ion has a

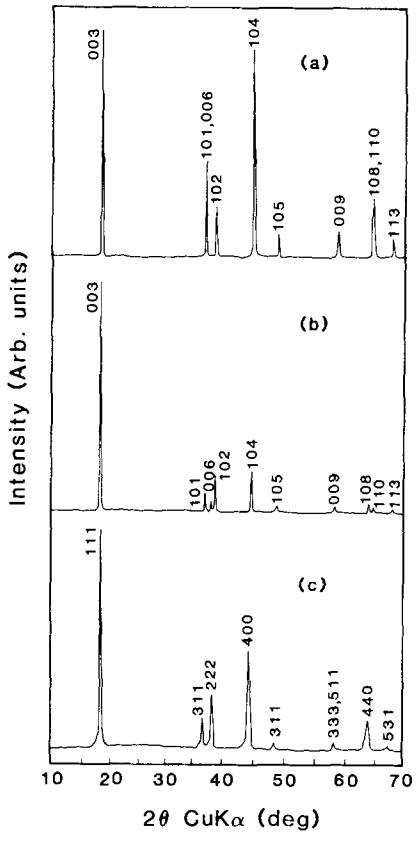

FIG. 2. X-ray powder diffraction patterns for (a) $Li_{0.96}Ni_{1.04}O_2$, (b) $Li_{0.58}Ni_{1.04}O_2$, and (c) $Li[Ni_2]O_4$.

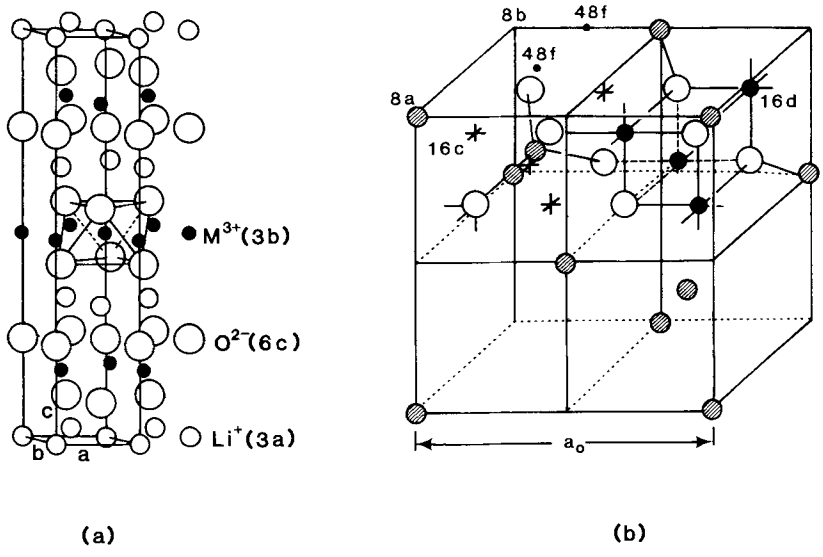

FIG. 3. Structures of (a) layered, ideal $LiMO_2$ (M = Ni) and (b) cubic spinel $A[M_2]O_4$.

preference for tetrahedral-site occupancy. The Ni^{2+}, Ni^{3+}, and Ni^{4+} ions all have a strong octahedral-site preference; however, displacement does occur above 250°C for $Li_{0.5}NiO_2$ in the transformation to the spinel $Li[Ni_2]O_4$.

Fig. 2(c) shows the X-ray powder-diffraction pattern for the spinel phase formed from $Li_{0.58}Ni_{1.04}O_2$ in the temperature range $250 < T < 300$°C. Of particular interest is the coalescence of the (108) and (110) reflections of the trigonal $R\bar{3}m$ phase, which indicates the transformation to a cubic phase. Based on a $2 \times 2 \times 2$ cubic rocksalt lattice, these reflections correspond to the crystallographically equivalent (440) and ($\bar{4}04$) spinel reflections in the cubic structure with space group $Fd3m$. The cubic lattice parameter of the spinel phase is $a = 8.190$ Å.

The trigonal ($R\bar{3}m$) layered structure of ideal $LiNiO_2$ is compared in Fig. 3 with the cubic ($Fd3m$) spinel structure. Formation of an $[M_2]O_4$ spinel framework from the trigonal layered phase $Li_{0.5}MO_2$ only requires a cooperative displacement of one quarter of the M atoms into neighboring Li-atom planes (*12*). A relatively high room-temperature Li^+-ion mobility in the interstitial space of an $[M_2]O_4$ spinel framework (*13*) allows the Li^+ ions to accommodate to the new M-atom ordering so as to maximize the electrostatic Madelung energy. Therefore transformation of $Li_{0.5}MO_2$ to form $Li[M_2]O_4$ only requires raising the temperature to where the interplanar displacements of the M atoms take place. In the system $Li_{1-x}VO_2$ with $0 < x < 0.5$, heating results in a disproportionation reaction into trigonal $LiVO_2$ and the spinel $Li[V_2]O_4$; heating $Li_{0.58}Ni_{1.04}O_2$ to 250–300°C appears to give only the spinel phase. The spinel $[V_2]O_4$ framework in $Li_{1+x}[V_2]O_4$ is stable over the range $0 \leq x \leq 1$ (*14*); we did not investigate the solid-solution range of $Li_{1+x}[Ni_2]O_4$.

3.2 Properties

The variation of resistance R with reciprocal temperature, Fig. 4, for $Li_{0.96}Ni_{1.04}O_2$ shows semiconductive behavior with an activation energy $E_a = 0.11$ eV below room temperature; above room temperature the activation energy drops to a small value.

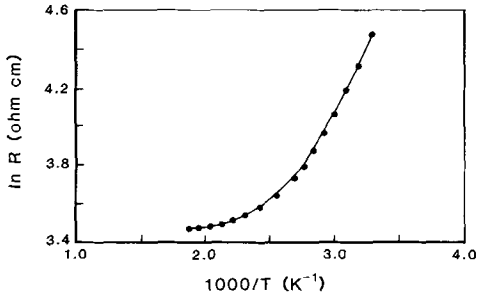

FIG. 4. Variation of resistance with reciprocal temperature for $Li_{0.96}Ni_{1.04}O_2$.

Given a mixed-valent configuration with E_F in the $Ni^{3+/2+}$ couple, the activation energy below room temperature is to be contrasted with metallic conductivity in the perovskite $LaNiO_3$ (*15*) and with a lack of any activation energy in the mobility of the mobile holes in $Li_xNi_{1-x}O$ having $x < 0.05$ (*3*). An $E_a = 0.11$ eV is typical for small-polaron conduction in a mixed-valent system, but small-polaron conduction is not expected for holes in a primarily O-2*p* valence band. Clearly an "ionic" model for the Ni–O bonding needs modification.

Resistance measurements were not made on the $Li_{0.96-x}Ni_{1.04}O_2$ samples; they are unstable above 250°C, which prevents the fabrication of sintered pellets. However, the temperature dependence of the resistance of a compacted-powder pellet of the spinel $Li[Ni_2]O_4$ was measured, Fig. 5. In this case the mixed-valent couple is $Ni^{4+/3+}$, yet this compound is also a semiconductor with an activation energy $E_a = 0.27$ eV. This value of E_a is like that of the small-polaron mobility in the spinel $Li[Mn_2]O_4$ (*16*), which has localized manganese moments and contains the strong Jahn–Teller ion Mn^{3+}; $Li_2[Mn_2]O_4$ is tetragonal due to a cooperative Jahn–Teller distortion of the Mn^{3+}-ion sites by a localized $^5E_g(t_2^3e^1)$ configuration (*17*).

The literature reports the temperature variation of the magnetic susceptibility of nominal $LiNiO_2$ (*18*) and also of isostructural $NaNiO_2$ (*19*). These data confirm an earlier deduction (*8*) that the Ni^{3+} ion is in its low-spin state, $^2E_g(t_2^6e^1)$ with $J \approx S = \frac{1}{2}$, which makes it potentially a strong Jahn–Teller ion like high-spin Mn^{3+}. Moreover, they also confirm the presence of ferromagnetic 90° Ni–O–Ni interactions within the (111) planes of nickel atoms, but there is no evidence of a cooperative Jahn–Teller distortion. The interplanar coupling between ferromagnetic Ni^{3+}-ion planes is dominated—in the case of $NaNiO_2$—by weak, antiferromagnetic Ni–O–O–Ni interactions; these are overwhelmed by a moderate external magnetic field to give a metamagnetic antiferromagnetic–ferromagnetic transition at a critical field $H_c = 17.6$ koe (*19*). In the case of nominal $LiNiO_2$, excess Ni are present in the Li-atom planes to provide antiferromagnetic 180° Ni–O–Ni interactions between a Ni^{2+} ion in a Li plane and its two neighboring ferromagnetic Ni-atom planes. Where these interactions dominate the interplanar coupling, nominal $LiNiO_2$ is a ferrimagnet with ferromagnetically coupled ferromagnetic Ni-atom planes ordered antiferromagnetically to the Ni^{2+} ions in the Li planes (*8, 18*).

Octahedral-site Ni^{2+} and low-spin Ni^{3+} and Ni^{4+} ions all contain filled t_2^6 configurations; these cannot participate in Ni–Ni in-

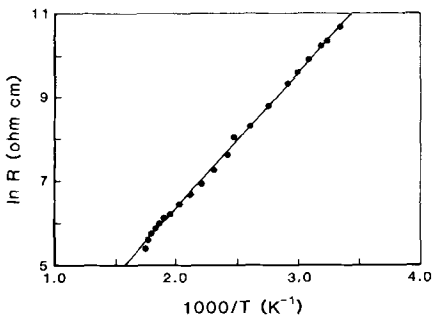

FIG. 5. Variation of resistance with reciprocal temperature for the spinel $Li[Ni_2]O_4$.

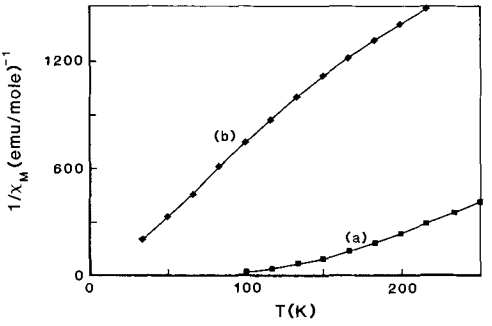

FIG. 6. Variation of inverse magnetic susceptibility with temperature for (a) $Li_{0.58}Ni_{1.04}O_2$ and (b) $Li_{0.32}Ni_{1.08}O_2$.

teractions across a shared octahedral-site edge. This situation leaves only 90° Ni–O–Ni nearest-neighbor interactions within the Ni-atom layers of the $R\bar{3}m$ structure and also within the $[Ni_2]O_4$ framework of the spinel structure. For a 90° Ni–O–Ni interaction, the partially filled e orbitals on neighboring Ni atoms are orthogonal to one another; therefore they experience a ferromagnetic direct-exchange (potential exchange) interaction (*1*). In the mixed-valent compositions, the ferromagnetic double-exchange interaction is inoperative where the mobile electrons are small polarons with an activated mobility (*1*). On the other hand, the 180° Ni^{2+}–O–Ni^{2+} superexchange interactions between half-filled e orbitals are strongly antiferromagnetic. In the absence of any Jahn–Teller distortion—static or dynamic—to order the single e electron of a Ni^{3+} ion among degenerate orbitals, the 180° Ni^{2+}–O–Ni^{3+} or Ni^{3+}–O–Ni^{3+} superexchange interactions are also antiferromagnetic. So too would be the weaker Ni–O–O–Ni superexchange interactions. These microscopic considerations are consistent with the macroscopic susceptibility data.

Figure 6 shows the temperature variation of the inverse magnetic susceptibility χ^{-1} of $Li_{0.32}Ni_{1.08}O_2$ and $Li_{0.58}Ni_{1.04}O_2$ over a limited temperature range below room temperature. The low-spin $Ni^{4+}(t_2^6e^0)$ ions are diamagnetic; only the Ni^{3+} ions contribute to the paramagnetic susceptibility. Although the temperature range is limited, the χ^{-1} vs T plot for $Li_{0.58}Ni_{1.04}O_2$ has a positive Weiss constant, indicative of the dominance of ferromagnetic interactions within the Ni-atom planes as in nominal $LiNiO_2$ and $NaNiO_2$. The corresponding curve for $Li_{0.32}Ni_{1.08}O_2$, on the other hand, has a negative Weiss constant, and the shape of the plot is typical for a ferrimagnet. We therefore conclude that the magnetic data provide clear—though indirect—evidence for the transfer of nickel to the Li-atom planes in $Li_{0.96-x}Ni_{1.04}O_2$ compositions having $x > 0.46$, but not where $x < 0.46$.

Figure 7 shows the χ^{-1} vs T plot for the spinel $Li[Ni_2]O_4$; in this structure the nickel atoms are well-ordered onto the octahedral sites of the $[Ni_2]O_4$ spinel framework, so only 90° Ni–O–Ni direct-exchange and weaker Ni–O–O–Ni superexchange interactions are operative. The paramagnetic susceptibility reveals a strongly positive Weiss constant consistent with strongly ferromagnetic 90° Ni–O–Ni direct-exchange interactions. However, the compound is not ferromagnetic; the susceptibility behaves like that of $Ge[Ni_2]O_4$ in which the weaker, antiferromagnetic Ni–O–O–Ni interactions

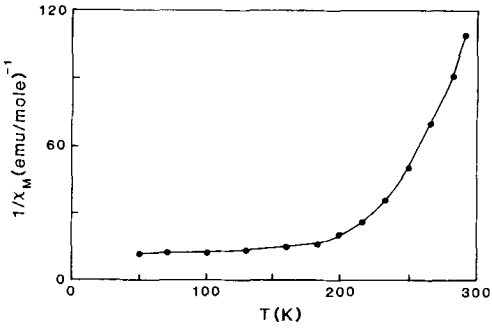

FIG. 7. Variation of inverse magnetic susceptibility with temperature for the spinel $Li[Ni_2]O_4$.

give rise to a spiral-spin configuration below the magnetic-ordering temperature (*20*). Whether this same situation applies to $Li[Ni_2]O_4$ is not certain; given the presence of diagmagnetic Ni^{4+} ions, the lack of ferromagnetism could, in this case, also be due to a lack of long-range magnetic order in the temperature range investigated.

What distinguishes these oxides from the perovskite $LaNiO_3$, which is metallic and Pauli paramagnetic (*15, 21*), is the presence of 90° Ni–O–Ni interactions rather than 180° Ni–O–Ni interactions. In $Li_{1-\delta}Ni_{1+\delta}O_2$, the presence of nickel in the Li-atom planes introduces some 180° Ni–O–Ni interactions; these are antiferromagnetic, and the resistance data for $Li_{0.93}NiO_2$ indicates that they provide low-resistance conduction paths that reduce the resistance and activation energy for conduction above room temperature.

4. Conclusions

$Li_{1-\delta-x}Ni_{1+\delta}O_2$ and the spinel $Li[Ni_2]O_4$ have been prepared for the first time by the chemical extraction—as opposed to electrochemical extraction—of lithium with the strong oxidizing agent NO_2PF_6.

Although spectroscopic data have led to the classification of NiO as having a charge-transfer energy gap, neither $Li_{1-\delta}Ni_{1+\delta}O_2$ nor the spinel $Li[Ni_2]O_4$ is metallic; they are both small-polaron semiconductors with the Fermi energy E_F lying in the $Ni^{3+/2+}$ redox band in the former case, the $Ni^{4+/3+}$ redox band in the latter case.

Moreover, the magnetic susceptibility data for $Li_{1-\delta-x}Ni_{1+\delta}O_2$ and the spinel $Li[Ni_2]O_4$ indicate the presence of low-spin Ni^{3+} and Ni^{4+} ions with a Ni^{3+}-ion magnetic moment corresponding to $S = \frac{1}{2}$ and $g \approx 2$. The only property that distinguishes these compounds from those having localized-electron magnetic moments is the lack of a cooperative Jahn–Teller distortion in nominal $LiNiO_2$ and $NaNiO_2$.

The width of the σ^* band associated with the σ-bonding orbitals of e parentage is given, in tight-binding theory, by $W \approx 2zb$, where z is the number of like nearest neighbors and the electron-transfer-energy integral $b \sim \varepsilon_\sigma(\psi_i, \psi_j)$ is proportional to the overlap integral (ψ_i, ψ_j) for crystal-field wave functions at sites $\mathbf{R}_i$ and $\mathbf{R}_j$. The 90° Ni–O–Ni interactions couple orthogonal crystal-field orbitals; orthogonality means a $b \approx 0$ and ferromagnetic direct-exchange interactions. On the other hand, the 180° Ni–O–Ni interactions in $LaNiO_3$ couple nonorthogonal crystal-field orbitals; nonorthogonality gives $b \sim \varepsilon_\sigma(\lambda_s^2 + \lambda_\sigma^2)$, where the λ_s and λ_σ are the covalent-mixing parameters between the Ni-e and O-s, p_σ orbitals, respectively. In NiO, where the Ni-e orbitals are half-filled, nonorthogonality gives antiferromagnetic Ni^{2+}–O–Ni^{2+} superexchange interactions, whereas in $LaNiO_3$ where Ni^{3+}–O–Ni^{3+} interactions occur, it gives a σ^* band broad enough to suppress spontaneous nickel atomic moments.

The data reported here provide clear evidence that the states at the Fermi energy not only retain the symmetry properties of the Ni-3d electrons of e character even for the $Ni^{4+/3+}$ couple, but also introduce a spontaneous Ni-atom atomic moment characteristic of strongly correlated crystal-field orbitals where the near-neighbor interactions between Ni atoms are 90° rather than 180° Ni–O–Ni interactions. These observations demonstrate that there is a transition from more ionic to more covalent Ni-e, O-p_σ bonding at octahedral-site nickel on oxidizing Ni^{2+} to Ni^{3+} and Ni^{4+}. Any ionic model for NiO does not apply to the oxides of nickel in higher oxidation states; holes introduced by oxidation do not occupy O-2p bands, but a $Ni^{3+/2+}$ or $Ni^{4+/3+}$ redox couple having the symmetry of the Ni-e orbitals and a massive Ni–O covalent mixing.

Acknowledgments

Financial support by the National Science Foundation, the Texas Advanced Research Program, and the R. A. Welch Foundation is gratefully acknowledged.

References

1. J. B. GOODENOUGH, *Prog. Solid State Chem.* **5,** 145 (1971).
2. J. ZAANEN, G. A. SAWATZKY, AND J. W. ALLEN, *Phys. Rev. Lett.* **55,** 418 (1985).
3. A. J. BOSMAN AND H. J. VAN DAAL, *Adv. Phys.* **19,** 1 (1970).
4. D. ADLER, *IBM J. Res. Dev.* **14,** 261 (1970).
5. H. BODE, K. DEHMELT, AND J. WITTE, *Electrochim. Acta* **11,** 1079 (1966).
6. M. G. S. R. THOMAS, W. I. F. DAVID, J. B. GOODENOUGH, AND P. GROVES, *Mater. Res. Bull.* **20,** 1137 (1985).
7. L. D. DYER, B. S. BORIE, JR., AND G. P. SMITH, *J. Am. Chem. Soc.* **76,** 1499 (1954).
8. J. B. GOODENOUGH, D. G. WICKHAM, AND W. J. CROFT, *J. Phys. Chem. Solids* **5,** 107 (1958).
9. J. B. GOODENOUGH, K. MIZUSHIMA, AND T. TAKEDA, *Jpn. J. Appl. Phys.* **19,** *Suppl.* **19–3,** 305 (1980).
10. R. WIZANSKY, P. E. RANCH, AND F. J. DISALVO, *J. Solid State Chem.* **81,** 203 (1989).
11. L. A. DE PICCIOTTO, M. M. THACKERAY, W. I. F. DAVID, P. G. BRUCE, AND J. B. GOODENOUGH, *Mater. Res. Bull.* **19,** 1497 (1984).
12. L. A. DE PICCIOTTO AND M. M. THACKERAY, *Mater. Res. Bull* **20,** 187 (1985).
13. M. M. THACKERAY, W. I. F. DAVID, AND J. B. GOODENOUGH, *Mater. Res. Bull* **17,** 785 (1982).
14. A. MANTHIRAM AND J. B. GOODENOUGH, *Can. J. Phys.* **65,** 1309 (1987); J. B. Goodenough, A. Manthiram, A. C. W. P. James, and P. Stroebel, *Mater. Res. Soc. Symp. Proc.* **B5,** 391 (1989).
15. J. B. GOODENOUGH AND P. M. RACCAH, *J. Appl. Phys.* **36,** 1031 (1965).
16. J. B. GOODENOUGH, M. M. THACKERAY, W. I. F. DAVID, AND P. G. BRUCE, *Rev. Chim. Miner.* **21,** 435 (1984).
17. M. M. THACKERAY, W. I. F. DAVID, P. G. BRUCE, AND J. B. GOODENOUGH, *Mater. Res. Bull.* **18,** 461 (1983).
18. J. P. KEMP, P. A. COX, AND J. W. HODBY, *J. Phys. Condens. Matter* **2,** 6699 (1990).
19. P. F. BONGERS AND U. ENZ, *Solid State Commun.* **4,** 153 (1966).
20. G. BLASSE AND J. F. FAST, *Philips Res. Rep.* **18,** 393 (1963).
21. J. P. KEMP AND P. A. COX, *Solid State Commun.* **75,** 731 (1990).